

*Short Communication*

## **Corrosion and Inhibition of P110 steel in 20% HCl Solution by Mannich Base Inhibitor**

Yanhua Zhu<sup>1</sup>, Liqiang Zhao<sup>1</sup>, Pingli Liu<sup>1\*</sup>, Peixin Chen<sup>1</sup>, Weidong Tao<sup>2</sup>

<sup>1</sup> State Key Laboratory of Oil & Gas Reservoir Geology and Exploitation Engineering, Southwest Petroleum University, Chengdu, Sichuan, 610500, China

<sup>2</sup> Fourth Oil Production Plant of Dagang Oilfield Company, Tianjin, 300280, China

\*E-mail: [zyhswpu@163.com](mailto:zyhswpu@163.com)

*Received:* 11 October 2018 / *Accepted:* 11 November 2018 / *Published:* 5 January 2019

---

The corrosion and inhibition behavior of P110 steel in 20% HCl solution with and without Mannich base inhibitor were investigated by electrochemical measurements and soaking experiments. The thermodynamic parameters demonstrated that the dissolution of P110 in HCl solution is an endothermic process. EIS studies indicated that the Mannich base inhibitor can effectively inhibit the corrosion reaction by forming an adsorption layer function as a barrier. Polarization curves indicated that it is mixed type inhibitor which can reduce anodic dissolution and cathodic hydrogen evolution reactions simultaneously.

---

**Keywords:** P110 steel, kinetic parameters, thermodynamic parameters, Mannich base, HCl solution

### **1. INTRODUCTION**

In recent years, the main oilfields have entered the decline stage and the experts and engineers are committed to increasing oil production by some effective measures[1]. Acidizing fracturing process is an effective and important method for enhancing oil production and is widely used at home and abroad [2,3]. Since the use of strong acid solution, usually HCl with high concentration, acidizing fracturing process will cause serious corrosion of tubular string, which brings tremendous losses to the safety of people's lives and property[4]. Many studies are working on how to control the corrosion, such as using less corrosive acids and corrosion resistant string, adding corrosion inhibitor and so on. P110 steel is an important steel in oil exploitation, however, its application is limited attributed to serious corrosion in acid solution[5-8]. In this work, the methods of static weight loss, potentiodynamic polarization curves, electrochemical impedance spectroscopy, surface morphology analysis and corrosion product analysis were used to study the corrosion behavior of P110 steel in 20% HCl solution (a commonly used acidizing

fluid) and the anti-corrosion protection mechanism of Mannich base corrosion inhibitor for P110 steel in this system. This study can expand the application of P110 steel in oilfield development.

## 2. EXPERIMENTAL

### 2.1. Materials

Benzoyl amine ( $\geq 99.0\%$ ), acetophenone ( $\geq 99.0\%$ ), cinnamaldehyde ( $\geq 99.0\%$ ), anhydrous ethanol ( $\geq 99.75\%$ ), HCl (approximately 36-38%) and acetone ( $\geq 99.5\%$ ) were obtained from Chengdu Kelon Chemical Reagent Company of China. The chemical composition of P110 steel specimens (50mm $\times$ 10mm $\times$ 3mm) used in this work is shown in Tab.1. The 20% HCl solution was prepared by diluting the saturated HCl with distilled water. The Mannich base inhibitor used in this study was a red-brown liquid which was synthesized by benzoyl amine, acetophenone and cinnamaldehyde through Mannich reaction in laboratory.

**Table 1.** Chemical composition of P110 steel wt%

| element | C    | Si   | Mn   | P     | S     | Cr  | V    | Al   | Ni   | Mo   | Cu  | Fe   |
|---------|------|------|------|-------|-------|-----|------|------|------|------|-----|------|
| content | 0.41 | 0.24 | 0.50 | 0.012 | 0.008 | 1.1 | 0.06 | 0.01 | 0.17 | 0.21 | 0.1 | Bal. |

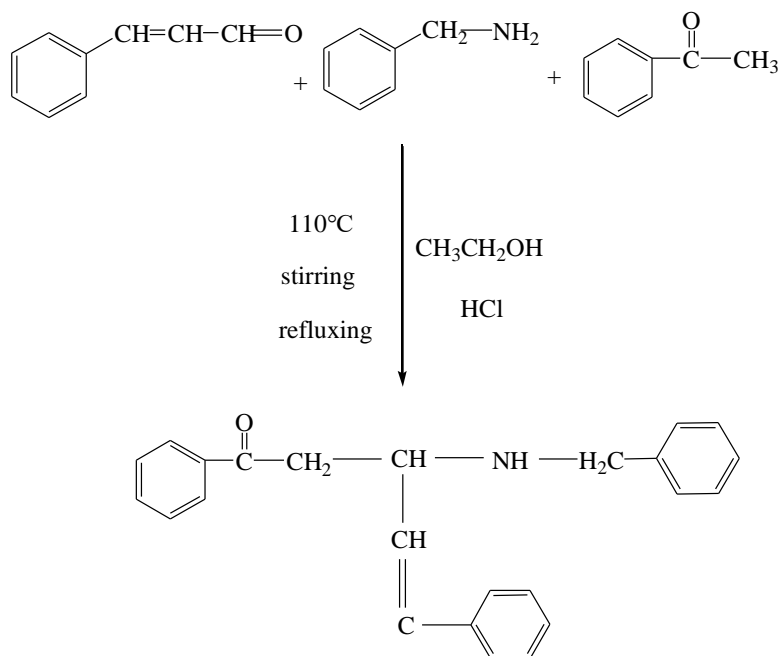
### 2.2. Instruments

HH-2K constant temperature water-bath ( $\pm 0.1^\circ\text{C}$ , Yuhua Instrument Company, Gongyi, China); ZF-9 electronic analytical balance ( $\pm 0.1$  mg, Shanghai Tetragonal Electronic Instrument Factory, China); CHI600 Electrochemical workstation (Chenhua Instrument Company, Shanghai, China); Scanning electron microscopy (SEM, JSM-7500F produced by JEOL) with X-ray energy dispersive spectroscopy (EDS).

### 2.3. Experimental method

#### 2.3.1 Synthesis of Mannich base

Benzoyl amine, acetophenone, cinnamaldehyde and anhydrous ethanol were placed in a 300-mL three-necked flask according to the volume concentration ratio of 1.2:1:1.2:1. After the addition of HCl to make pH approximately 3-4, the mixture was refluxed for 8 hours with stirring at  $110^\circ\text{C}$  and then cooled. The synthetic route and molecular structure are shown in Scheme 1.



**Scheme 1.** Synthetic route and molecular structure of Mannich base

### 2.3.2. Corrosion experiment of weight loss method

The fresh P110 steel was washed with acetone and ethyl alcohol, dried in desiccators and then weighed accurately. The soaking experiment was carried out by immersing P110 steel in 20% HCl for 4 hours at different temperatures with or without inhibitor. Then, the P110 steel was taken out, washed with distilled water, acetone and anhydrous ethanol, dried in desiccators and reweighed. The corrosion rate ( $C_R$ ) was calculated using equation (1):

$$C_{Ri} = \frac{10^6 \Delta m_i}{A_i \Delta t} \quad (1)$$

where  $C_{Ri}$  ( $\text{g}\cdot\text{m}^{-2}\cdot\text{h}^{-1}$ ) is the corrosion rate of each steel specimen,  $A_i$  ( $\text{mm}^2$ ) is the surface area of steel coupon,  $\Delta t$  (h) is the time of corrosion reaction and  $\Delta m_i$  (g) is the weight loss of the steel specimen. The corrosion inhibition efficiency ( $IE$ ) of Mannich base inhibitor is calculated using equation (2):

$$IE = \frac{\bar{C}_{R0} - \bar{C}_R}{\bar{C}_{R0}} \times 100\% \quad (2)$$

where  $\bar{C}_{R0}$  ( $\text{g}\cdot\text{m}^{-2}\cdot\text{h}^{-1}$ ) and  $\bar{C}_R$  ( $\text{g}\cdot\text{m}^{-2}\cdot\text{h}^{-1}$ ) are the average corrosion rate in the absence and presence of the inhibitor, respectively.

### 2.3.3. Electrochemical measurements

Potentiodynamic polarization and electrochemical impedance spectroscopy (EIS) are two techniques which were used to study the electrochemical corrosion behavior of P110 steel in 20% HCl solution with and without corrosion inhibitor. All electrochemical experiments were performed at 333K in an electrochemical cell with three electrodes connected to electrochemical workstation. In which, the

standard calomel electrode (SCE) was used as reference electrode, platinum electrode was used as an auxiliary electrode and steel of 1.0cm<sup>2</sup> (10mm×10mm) was the working electrode. All electrochemical experiments were measured after reaching a steady open circuit potential. Potentiodynamic polarization curves were obtained by changing the electrode potential automatically from -300 to + 300mV versus  $E_{oc}$  at a scan rate of 0.1mV·s<sup>-1</sup>.

The inhibition efficiency ( $IE_p$ ) on the corrosion of steel was calculated using equation (3):

$$IE_p = \frac{I_{corr} - I'_{corr}}{I_{corr}} \times 100\% \quad (3)$$

where  $I_{corr}$  (mA·cm<sup>-2</sup>) and  $I'_{corr}$  (mA·cm<sup>-2</sup>) are the corrosion current density of steel specimens in the absence and presence of inhibitor, respectively.

Impedance measurements were carried out using AC signals of amplitude 5mV peak to peak at the open-circuit potential ( $E_{oc}$ ) in the frequency range from 10<sup>5</sup>Hz to 10<sup>-2</sup>Hz. The inhibition efficiency ( $IE_E$ ) on the corrosion of steel was calculated using equation (4):

$$IE_E = \frac{R'_{corr} - R_{corr}}{R'_{corr}} \times 100\% \quad (4)$$

where  $R_{corr}$  (Ω) and  $R'_{corr}$  (Ω) are the charge transfer resistance of steel specimens in the absence and presence of inhibitor, respectively.

### 2.3.4. Surface analysis of P110 steel

The microstructure of P110 steel surface after immersing in 20% HCl solution with and without corrosion inhibitor was obtained using a scanning electron microscope. The elemental composition and content of corrosion products on P110 steel surface were obtained using EDS analysis.

## 3. RESULTS AND DISCUSSION

### 3.1. The corrosion inhibition efficiency of Mannich base

#### 3.1.1. Effect of inhibitor concentration

In order to select the optimal concentration of Mannich base, weight loss measurements were performed in 20% HCl solution for 4h at 333K. The corrosion rates and inhibition efficiencies calculated for various concentrations of Mannich base inhibitor are shown in Tab.2.

**Table 2.** Corrosion rate and inhibition efficiency for P110 steel in 20% HCl solution with Mannich base inhibitor with different concentrations obtained by weight loss method at 333K for 4h

| $C_{inh}(wt\%)$                           | 0      | 0.5   | 1.0   | 1.5   | 2.0   | 2.5   | 3.0   | 3.5   | 4.0   |
|---|--------|-------|-------|-------|-------|-------|-------|-------|-------|
| $\bar{C}_R (g \cdot m^{-2} \cdot h^{-1})$ | 373.67 | 17.52 | 4.16  | 2.37  | 1.15  | 0.72  | 0.61  | 0.60  | 0.59  |
| IE(%)                                     | -      | 95.31 | 98.89 | 99.37 | 99.69 | 99.81 | 99.84 | 99.84 | 99.84 |

From Tab.2, it can be found that corrosion inhibition efficiency increased and the corrosion rate decreased considerably with the increasing of inhibitor concentration. This may be attributed to the increased adsorption and coverage of Mannich base molecular on P110 steel surface[9,10]. The inhibition behavior of Mannich base inhibitor may be attributed to a compact and coherent film formed on P110 steel and reduced chemical attacks of H<sup>+</sup> and Cl<sup>-</sup>. The corrosion rate of P110 steel is 2.37g·m<sup>-2</sup>·h<sup>-1</sup> which has already reached the requirement of acidification when the concentration of Mannich base is 1.5% (wt.%). Therefore, all of the concentration of Mannich base inhibitor is 1.5% in the following experiments.

### 3.1.2. Effect of temperature

In order to study the effect of temperature on corrosion and inhibition characteristic of Mannich base inhibitor, weight loss measurements were performed at different temperatures from 323 to 363K with and without 1.5% Mannich base inhibitor and the results are shown in Tab.3. As detected from Tab.3, corrosion rate increased with increasing of temperature in studied temperature range. Simultaneously, the inhibition efficiency of 1.5% Mannich base decreased mildly with increasing of temperatures in studied temperature range but still more than 99%. The stability of inhibition efficiency implies that the Mannich base inhibitor has good temperature resistance and can effectively inhibit the corrosion of P110 steel in a wide temperature range adopted in this experiment.

**Table 3.** Corrosion rate and inhibition efficiency of P110 steel in 20% HCl solution with 1.5% Mannich base at different temperatures from weight loss method for 4h

| T(K)  | system    | 323    | 333    | 343    | 353     | 363     |
|---|-----------|--------|--------|--------|---------|---------|
| $\bar{C}_R$ (g·m <sup>-2</sup> ·h <sup>-1</sup> ) | blank     | 193.26 | 373.67 | 586.58 | 1009.89 | 1639.65 |
|   | inhibitor | 1.06   | 2.37   | 4.22   | 8.79    | 15.25   |
| IE(%)   | inhibitor | 99.45  | 99.37  | 99.28  | 99.13   | 99.07   |

The relationship between corrosion rate and temperature can be expressed by Arrhenius equation and its transition state equation[11,12]:

$$\ln(C_R) = \frac{-E_a}{RT} + \ln A \tag{4}$$

$$C_R = \frac{RT}{Nh} \exp\left(\frac{\Delta S_a^*}{R}\right) \exp\left(-\frac{\Delta H_a^*}{RT}\right) \tag{5}$$

where  $E_a$  is apparent activation energy,  $A$  is the pre-exponential factor,  $\Delta H_a^*$  is the apparent enthalpy of activation,  $\Delta S_a^*$  is the apparent entropy of activation,  $h$  is Planck's constant ( $6.626 \times 10^{-34}$ ) and  $N$  is the Avogadro number ( $6.02 \times 10^{23}$ ), respectively.

The apparent activation energy and pre-exponential factors of 1.5% Mannich base for P110 steel can be calculated by linear regression between  $\ln C_R$  and  $1/T$ , the results were shown in Tab.4. The plots obtained are straight lines and the slop of straight line gives its apparent activation energy and the intercept gives its pre-exponential factor.

**Table 4.** Thermodynamic activation parameters for P110 steel in 20% HCl with and without 1.5% Mannich base inhibitor

| system             | $E_a$<br>(kJ·mol <sup>-1</sup> ) | $A$<br>(mg·cm <sup>-2</sup> ) | $\Delta H_a^*$<br>(kJ·mol <sup>-1</sup> ) | $\Delta S_a^*$<br>(J·mol <sup>-1</sup> ·K <sup>-1</sup> ) |
|--------------------|----------------------------------|-------------------------------|---|---|
| HCl                | 50.00                            | $2.53 \times 10^{10}$         | 24.50                                     | -112.108  |
| HCl + Mannich base | 96.28                            | $8.53 \times 10^{14}$         | 93.40                                     | 31.42   |

Tab.4 showed that in presence of Mannich base inhibitor, activation energy increased compared to the free acid solution. The increase in  $E_a$  could be interpreted as the physical adsorption which occurs in the first stage[13-15]. From Tab.4, it can be seen that for P110 steel specimens,  $E_a$  is higher for inhibited solution than free acid solution. It is clear from equation (4) that the higher  $E_a$  and lower  $A$  lead to the lower corrosion rate. In general, the effect of  $E_a$  on steel corrosion is much higher than that of  $A$  on steel corrosion. In the present study, the combined effect of  $E_a$  and  $A$  results in increase of corrosion rate with temperature.

The positive values of  $\Delta H_a^*$  show that the dissolution reaction of P110 steel in HCl solution is an endothermic process, which indicates that the corrosion rate increases with the increasing temperature. The different values of  $\Delta S_a^*$  mean that the perplexity of molecular distribution on steel surface changed in different levels with different dissolution process.

### 3.2. Electrochemical measurements

#### 3.2.1. Polarization curve analysis

Polarization curves of P110 steel electrode in 20% HCl solution with and without 1.5% Mannich base at 333K are shown in Fig.1. The Polarization parameters of P110 steel specimens in 20% HCl solution with and without 1.5% Mannich base at 333K are summarized in Tab.5.

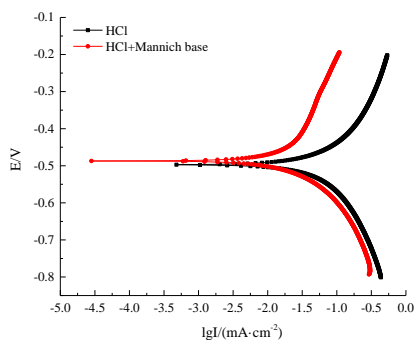


**Figure 1.** Polarization curves for P110 steel in 20% HCl solution with and without 1.5% Mannich base inhibitor at 333K

**Table 5.** Polarization parameters of P110 steel in 20% HCl solution with and without 1.5% Mannich base inhibitor at 333K

| inhibitor    | $E_{corr}(mV)$ | $b_a(mV/dec)$ | $-b_c(mV/dec)$ | $I_{corr}(\mu A/cm^2)$ | $IE_p$ |
|--------------|----------------|---------------|----------------|------------------------|--------|
| blank        | -497           | 97            | 102            | 358                    | -      |
| Mannich base | -487           | 94            | 96             | 6.5                    | 98.18  |

It can be found that the corrosion current density of steel in the system with Mannich base reduced and the corrosion rate decreased. According to the literatures[16,17], it has been reported that if the displacement in  $E_{corr}$  in the presence of inhibitor is less than 85 mV, the inhibitor can be classified as a mixed type. According to the data from Tab.5, it can conclude that this Mannich base inhibitor acts as a mixed type inhibitor and has more influence on anodic polarization plots. The values of  $b_a$  and  $b_c$  exhibit no obvious changes, which suggests that the inhibition effect comes from the reduction of the reaction area on the corroding metal surface.

3.2.2. AC Impedance analysis

Fig.2 and Fig.3 show that the steels' electrochemical impedance spectrums and Bode curves are in the same shapes after immersing in 20% HCl solution with and without Mannich base inhibitor, which indicated that the presence of Mannich base inhibitor did not change the electrochemical behavior of steel when the corrosion system reaches equilibrium, thus it can come to the conclusion that the Mannich base inhibitor cannot change the corrosion mechanism of steel although it can effectively increase the corrosion resistance. This conclusion is highly agreement with that of result of polarization curves.

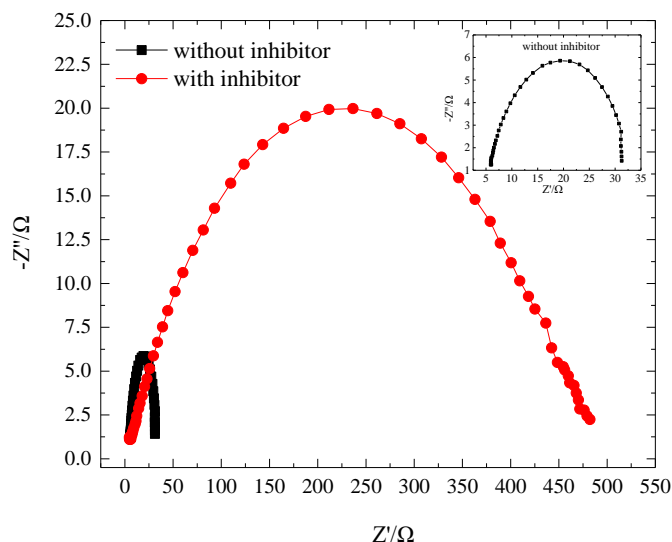


**Figure 2.** Nyquist curves for P110 steel immersed in 20% HCl solution with and without 1.5% Mannich base inhibitor at 333K

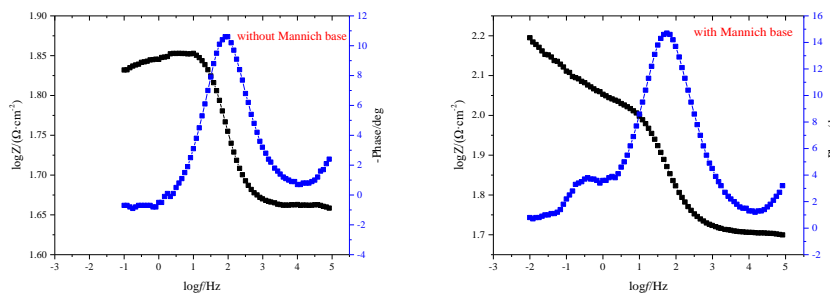


**Figure 3.** Bode curves for P110 steel immersed in 20% HCl solution with and without 1.5% Mannich base inhibitor at 333K

It can be found that all the impedance spectra displayed in Fig.2 reveal a single depressed capacitive semicircle, which denotes that the dissolution process is related to the charge transfer process[18]. It also can be seen that these impedance loops are not perfect semicircles, which can be termed as frequency dispersion effect as a result of the roughness and inhomogeneity of the metal electrode surface[19]. The Bode curves for different steel immersed in 20% HCl solution with and without Mannich base inhibitor indicate that only one phase peak at the middle frequency range can be observed, confirming that there is only one time constant[20,21]. Various impedance parameters and inhibition efficiency were calculated and listed in Tab.6. It can be seen that the  $R_p$  value increases while  $C_{dl}$  value decreases with addition of Mannich base. These results indicated that the Mannich base inhibitor molecules acted by adsorption on the steel/solution surface and formed a layer which can effectively prevent the directly contact between steel surface and corrosive medium, so as to decrease the corrosion rate of P110 steel[22,23].

**Table 6.** EIS parameters of P110 steel specimens in 20% HCl solution with and without 1.5% Mannich base inhibitor at 333K

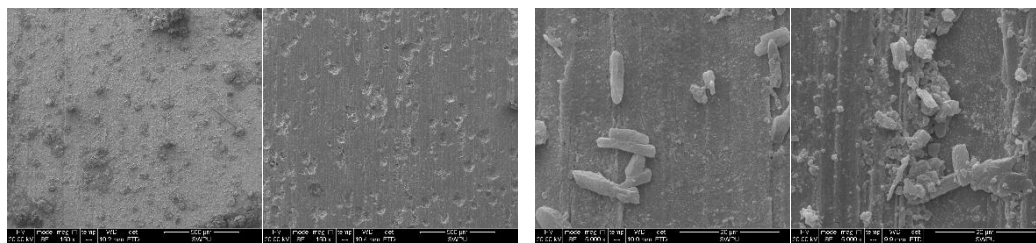
| inhibitor    | $R_p(\Omega \cdot \text{cm}^2)$ | $f_{\text{max}}(\text{Hz})$ | $C_{dl}(\mu\text{F} \cdot \text{cm}^{-2})$ | $IE_E$ |
|--------------|---------------------------------|-----------------------------|--|--------|
| blank        | 40                              | 5.62                        | 214.22                                     | -      |
| Mannich base | 728                             | 26.10                       | 46.12                                      | 94.51  |

### 3.3. Surface analysis of P110 steel: SEM and EDS

#### 3.3.1. Corrosion morphologies

Fig.4 shows the scanning electron micrographs of P110 steel surface after immersing in 20% HCl solution with and without Mannich base.





(a) steel surface without Mannich base (b) steel surface with Mannich base

**Figure 4.** Scanning electron micrographs of P110 steel surface after immersing in 20% HCl solution with and without 1.5% Mannich base inhibitor for 4h at 333K

It can be seen that the surface was damaged substantially and many pits with large diameter and deepness are visible after immersing in 20% HCl solution without Mannich base inhibitor for 4h at 333K. It is found to be covered with a protective film of compounds uniformly spread over the P110 steel surface after immersing in 20% HCl with Mannich base inhibitor. The protective film that prevents the attack of H<sup>+</sup> and Cl<sup>-</sup> on the metal may be formed due to adsorption of the inhibitor molecules on the steel surface.

3.3.2 Component of corrosion products

It can be observed from Tab.7 that the major elements of product are the main elements of steel and corrosion inhibitor such as C, O, Fe and Mn. The content of element C in Mannich base system increased very evidently when compared with those without Mannich base, which indicated that the major element of Mannich base involved in product formation. Moreover, the content of element Fe and Mn in Mannich base system decreased, which indicated that less steel was dissolved in inhibitor system. The results of EDS test confirmed that the corrosion inhibitors formed a layer of protective membrane which can prevent the contact of Cl<sup>-</sup> with steel surface, and then inhibited the corrosion of steel in corrosive solution.

**Table 7.** Elemental content of P110 steel surface after immersing in 20% HCl with and without 1.5% Mannich base inhibitor for 4h at 333K

| inhibitor    | content | C     | O     | Fe    | Mn   |
|--------------|---------|-------|-------|-------|------|
| blank        | Wt%     | 10.54 | 4.38  | 82.94 | 2.15 |
|              | At%     | 32.79 | 10.24 | 55.51 | 1.46 |
| Mannich base | Wt%     | 38.47 | 7.33  | 54.20 | -    |
|              | At%     | 69.15 | 9.89  | 20.96 | -    |

Notes: Wt%: the relative mass percentage of the elements; At %: the relative atomic number percentage of the elements.

### 3.4. Inhibiting mechanism of Mannich base inhibitor

From the results obtained from weight loss and electrochemical measurements, it was concluded that the Mannich base inhibit the corrosion of P110 steel in 20% HCl solution by adsorption at metal/solution interface. It is general assumption that the adsorption of organic inhibitors at the metal surface interface is the first step in the mechanism of the inhibitor action. The inhibition of active dissolution of the metal is due to the adsorption of the inhibitor molecules on the metal surface forming a protective film. The inhibitor molecules can be adsorbed onto the metal surface through electron transfer from the adsorbed species to the vacant electron orbital of low energy in the metal to form a co-ordinate type link.

## 4. CONCLUSION

(1) The inhibiting effect of Mannich base increases with increase of inhibitor concentration and decreases with increase of temperature.

(2) Electrochemical tests indicated that the Mannich base inhibitor is a kind of mixed type inhibitor which can inhibit the anodic and cathodic corrosion reaction simultaneously and do not change the corrosion mechanism of P110 steel in 20% HCl solution.

(3) The presence of Mannich base in the solution increased the value of the apparent activation energy, hence increased the difficulty of metal dissolution.

## ACKNOWLEDGEMENTS

The work is supported by National Science and Technology Major Project of the Ministry of Science and Technology of China “High Efficiency Oil Production and Supporting Technology Demonstration on Bohai Oilfield” (No. 2016ZX05058-003).

## References

1. Y.Y. Lv and Y. Wang, *Petrol. Tubul. Goods Instrum.*, 1(2015)5.
2. Z.Q. Qu, N. Qi, Z.Q. Wang, H. Xu and Y.Z. Wang, *Petrol. Geology Recov. Effic.*, 13(2006)93.
3. S.J. Zhou, X.H. Guo and S.Z. Du, *Corros. Sci. Protect. Technol.*, 26(2014)469.
4. Q. Quan, Z.Z. Hao, L. Li, W. Bai, Y.J. Liu and Z.T. Ding, *Corros. Sci.*, 51(2009)569.
5. X. Liu, J.S. Yang, Y.P. Liu, X.Y. Ji, Y. Lu and Y.Z. Yuan, *Surf. Rev. Lett.*, 24(2017)1750024.
6. N.M. Lin, P. Zhou and H.W. Zhou, *Int. J. Electrochem. Sci.*, 10(2015)2694.
7. H.B. Wu, L.F. Liu, L.D. Wang and Y.T. Liu, *J. Iron Steel Res. Int.*, 21(2014)76.
8. J.L. Li, H.X. Ma, S.D. Zhu, C.T. Qu and Z.F. Yin, *Corros. Sci.*, 86(2014)101.
9. A.K. Singh and M.A. Quraishi, *J. Appl. Electrochem.*, 40(2010)1293.
10. J.O. Bockris and D. Drazic, *Electrochim. Acta*, 7(1962)293.
11. E.A. Noor and A. H. Al-Moubaraki, *Mater. Chem. Phys.*, 110(2008)145.
12. L. Larabi, O. Benali and Y. Harek, *Mater. Lett.*, 61(2007)3287.
13. T. Szauer and A. Brandt, *Electrochim. Acta*, 26(1981)1257.
14. P.K. Ghosh, D.K. Guhasarkar and V.S. Gupta, *Brit. Corros. J.*, 18(2013)187.
15. M. Abdallah, *Corros. Sci.*, 44(2002)717.
16. A.A.F. Sabirneeza and S. Subhashini, *Inter. J. Ind. Chem.*, 5(2014)111.

17. E.S. Ferreira, C. Giacomelli, F.C. Giacomelli and A. Spinelli, *Mater. Chem. Phys.*, 83(2004)129.
18. P.K. Ghosh, D.K. Guhasarkar and V.S. Gupta, *Brit. Corros. J.*, 18 (2013) 187.
19. K. Tebbji, B. Hammouti, H. Oudda, A. Ramdani and M. Benkadour, *Appl. Surf. Sci.*, 252 (2005) 1378.
20. Y. Abboud, A. Abourriche, T. Saffaj, M. Berrada and M. Charrouf, *Appl. Surf. Sci.*, 252 (2006) 8178.
21. D.A. Lopez, T. Perez, S. N. Simison, *Mater. Design*, 24 (2003) 561.
22. D.A. Lopez, T. Perez and S.N. Simison, *Mater. Design*, 24(2003)561.
23. L.D. Paolinelli, T. Perez and S.N. Simison, *Corros. Sci.*, 50(2008)2456.

© 2019 The Authors. Published by ESG ([www.electrochemsci.org](http://www.electrochemsci.org)). This article is an open access article distributed under the terms and conditions of the Creative Commons Attribution license (<http://creativecommons.org/licenses/by/4.0/>).